EXCITATIONS OF THE EARTH'S CHANDLER WOBBLE AND LENGTH OF DAY BY THE SOUTHERN OCEAN

E. NAGHIBI[1], C. Delizo-Salabit[2], S. KARABASOV[3]

[1] School of Architecture, Computing and Engineering, University of East London - United Kingdom - e.naghibi@uel.ac.uk

[2] Ernst & Young UK - United Kingdom

[3] School of Engineering and Materials Science, Queen Mary University of London - United Kingdom - s.karabasov@qmul.ac.uk

ABSTRACT. In this paper, the effect of Southern Ocean on Chandler wobble and length of day excitations is investigated. To this end, the motion terms of excitations are calculated using the primitive equation ocean model, HYCOM (HYbrid Coordinate Ocean Model). The resulting excitations are analysed in time and frequency domains and compared to the previous studies for regional oceanic excitations of Chandler wobble and length of day. The excitations caused by the Southern Ocean are also compared with those caused by the global oceans in the same general circulation ocean model, HYCOM. Our results suggest that, amongst all oceanic regions, the Southern Ocean is a key contributor to both Chandler wobble and length of day excitations. The predicted excitations caused by the global oceans are also compared with geodetic observation of the Chandler wobble and length of day after subtraction of mass terms estimated from GRACE (Gravity Recovery and Climate Experiment) satellite gravimetry data.

1. INTRODUCTION

Geophysical sources of excitation for the Earth's polar motion and length of day in different time scales have always been an interesting question for geodynamicists. Starting with polar motion excitation at small time scales , ocean tides are reported to influence polar motion in sub-daily timescales [1, 2]. Angular momentum exchanges between the core and the mantle also affect polar motion at these timescales [1]. At intraseasonal timescales, most dominant excitation source is from atmospheric and oceanic processes, explaining roughly 65% and 71% of the observed excitation variance, between 1980 – 2000 and 1993 – 2000 respectively [3]. Forced annual wobble excitation is predominantly caused by seasonal shifting of air mass [4-6]. On the other hand, for the Chandler wobble excitation, ocean bottom pressure is the most significant mechanism [7], having 1.5 times more power that atmospheric surface pressure and 8 times more power than oceanic currents. The combined contribution of the atmospheric and oceanic processes account for 1.2 times the observed Chandler wobble from 1980 to 2000 [3] with atmospheric and ocean pressure variations being the most dominant mechanism. This highlights the significance of damping in Chandler wobble motion. Aoyama et al. [8] however noted that atmospheric wind and surface pressure were the dominant mechanisms in the same time period with wind being the main component. This is further supported by work done by Brzezinski et al. [9] which reported atmospheric wind and surface pressure contributing to 80% of the total excitation from atmospheric and oceanic processes in similar time periods.

Moving on to LOD excitations, at diurnal timescales, ocean tides are the predominant excitation mechanism providing up to 90% contribution [10]. Schindelegger et al. [11] discovered El Nino - Southern Oscillation to be the main perturbation for diurnal cycle characteristics in the troposphere. Atmospheric and oceanic processes cause 92% of the observed LOD variations in

intraseasonal time scales from 1980 – 2000 and 1992 – 2000 [12]. Atmospheric processes significantly dominate oceanic processes, with motion effects contributing more than the pressure. However,, ocean bottom pressure and currents are also shown to be effective in these time scale [13]. Effects of upper atmospheric winds (10hPa to 0.3hPa) were analysed at the same timescales and were shown to be weaker than lower atmospheric winds (ground to 10hPa), however, they still had a greater effect than ocean contributions. Rosen et al. [14], over a 2 - year sample, has also deduced that tropospheric and stratospheric winds can fully account for seasonal, nontidal variations in LOD. Leading up to seasonal timescales, ocean excitation contributions become more significant, with large scale variations in ocean water mass and water on land being responsible [18]. Lambeck Hopgood [15] find that zonal wind and body tides dominate semi-annual timescales with the remaining 10% contribution coming from oceanic currents and hydrologic processes, especially associated with the Antarctic circumpolar current in the Southern Ocean. In interannual timescales [12] atmospheric and oceanic processes explain around 88% of observed variations, with atmospheric processes having a larger contribution than oceanic processes.

The Southern Ocean, embracing Antarctic Circumpolar Current (ACC),the strongest current on the Earth, is an important player in the climate system. Given the strength of currents in the Southern Ocean, the resulting angular momentum for this region is one of the key contributors in overall oceanic angular momentum. Hence, as suggested by previous articles [16-19], the Southern Ocean has a dominant role in the motion term of excitation for polar motion and length of day. In this paper, the general circulation ocean model, HYCOM, is deployed to investigate the regional effect of the Southern Ocean on the Earth's polar motion and length of day. As a high resolution general circulation model with realistic continent boundaries and bottom topography, multiple layers in depth and wind forcing adopted from general circulation atmospheric models, HYCOM is capable of predicting ocean dynamics with high fidelity [20]. The angular momentum calculated from HYCOM simulations have a very rich temporal variability, and hence, have a larger effect on the Earth dynamics than low fidelity ocean models, such as the quasi-geostrophic models [21, 22] and reduced-order ocean dynamics models [23, 24].

The paper is structured as follows: the governing equations for polar motion and length of day as well as HYCOM governing equations are presented in the methods section with typical HYCOM simulation results illustrated in the end of the section. Predicted values for angular momentum components and change in length of day for global oceans and the isolated region of the Southern Ocean are shown in the results section and conclusions are discussed in the last section.

2. METHODS

In this study, the polar motion and length of day excitation functions caused by oceanic angular momentum are calculated using the general circulation model, HYCOM.

2.1 Polar motion and length of day equations

Polar motion and length of day equations are given as

$$\begin{aligned} \frac{\dot{m}_1}{\sigma_0} + m_2 &= \frac{\Omega^2 c_{23} - \Omega \dot{c}_{13} + \Omega h_2 - \dot{h}_1}{\Omega^2 (C-A)} \frac{k_s}{k_s - k} = \phi_2 \\ \frac{\dot{m}_2}{\sigma_0} - m_1 &= -\frac{\Omega^2 c_{13} + \Omega \dot{c}_{23} + \Omega h_1 + \dot{h}_2}{\Omega^2 (C-A)} \frac{k_s}{k_s - k} = -\phi_1 \\ \dot{m}_3 &= \frac{-\Omega \dot{c}_{33} - \dot{h}_3}{\Omega C} \left(1 + \frac{4}{3} \frac{k}{k_s} \frac{C-A}{C}\right)^{-1} = \phi_3 \end{aligned} \tag{1}$$

where m_1 and m_2 are polar motion and m_3 is the length of day component, Ω is the Earth's spin rate, k is the Love number, k_s is the secular Love number and σ_0 is the Chandler frequency. h_i are relative angular momentum components, c_{ij} are the perturbations of the Earth's moment of inertia with A and C as the main components and ϕ_i are the excitation function componets [25].

2.2 HYCOM governing equations

To calculate oceanic excitation of polar motion and length of day, we use solutions from a general ocean circulation HYCOM (HYbrid Coordinate Ocean Model). The model simulation results are downloaded from the HYCOM data portal (hycom.org), where they had been interpolated to z-level coordinates. HYCOM governing equations consist of the conservation laws for momentum, temperature, salinity and mass, as well as the equation of state:

$$\begin{aligned}
&\tfrac{\partial \mathbf{v}}{\partial t} + (\mathbf{v}.\nabla)\,\mathbf{v} + 2\boldsymbol{\omega} \times \mathbf{v} = -\tfrac{\nabla P}{\rho} + \tfrac{\nabla.\boldsymbol{\tau}}{\rho},\\
&\tfrac{\partial T}{\partial t} + \nabla.\,(T\mathbf{v}) = \nabla.\,(\kappa\,\nabla T) + F^{T},\\
&\tfrac{\partial S}{\partial t} + \nabla.\,(S\mathbf{v}) = \nabla.\,(\kappa\,\nabla S) + F^{S},\\
&\nabla.\mathbf{v} = 0,\\
&\rho = \rho\,(T, S, P)\,,
\end{aligned} \tag{2}$$

where $\mathbf{v} = (u, v, w)$ is the velocity vector, $\boldsymbol{\omega}$ is the Earth's angular velocity vector, P is pressure, and $\boldsymbol{\tau}$ is a stress tensor including viscosity. T and S are temperature and salinity while F^T and F^S are the corresponding source terms in their conservation equations, κ is diffusivity tensor and ρ is the density. The horizontal resolution in HYCOM is 1/12 degree in the longitude and latitude and the model includes 41 isopycnal layers. The hybrid coordinate is isopycnal in the open, stratified ocean while it reforms to terrain-following coordinates in shallow coastal regions and to z-level coordinates in the mixed layer and unstratified seas. The atmospheric wind forcing in HYCOM is time-dependent and is generated by atmospheric general circulation models such as NAVGEM (Navy Global Environmental Model) [20].

Typical ocean simulation results by HYCOM are illustrated in figures 1-4. Figures 1 and 3 show instantaneous distributions of zonal and meridional velocity components in HYCOM simulations with the Southern Ocean region depicted in a rectangular box. Figure 2 displays time and layer averaged distribution of zonal velocity in the Southern Ocean region as well as its zonally averaged profile versus the meridional coordinate. Similarly, in figure 4 time and layer average distribution of meridional velocity is shown in the Southern Ocean region as well as its meridionally averaged profile versus the zonal coordinate. Time averaging is performed in the 5-year period from December 2013 to December 2018 based on 10-day sampled snapshots.

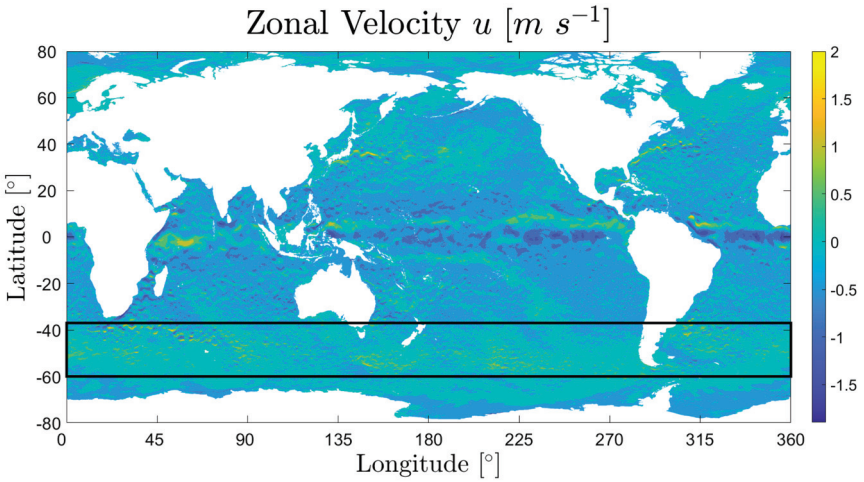

Figure 1: Instantaneous zonal velocity distribution in HYCOM simulations for the top isopycnal layer. The Southern Ocean region is displayed in a rectangular window.

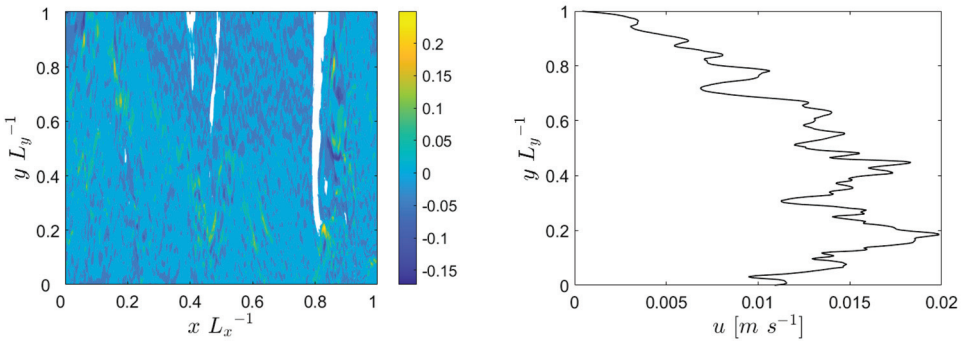

Figure 2: Time and layer averaged zonal velocity distribution (left); time, layer and zonally-averaged zonal velocity profile vs meridional coordinate (right) for the Southern Ocean region in HYCOM simulations.

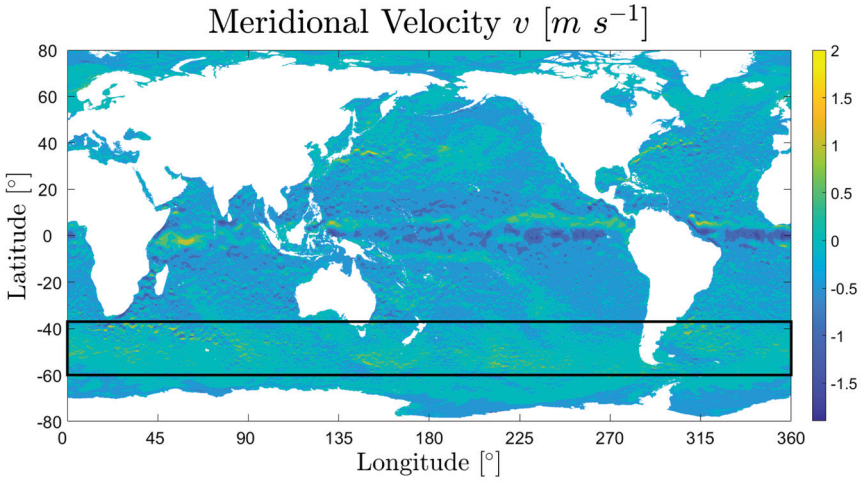

Figure 3: Instantaneous meridional velocity distribution in HYCOM simulations for the top isopycnal layer. The Southern Ocean region is displayed in a rectangular window.

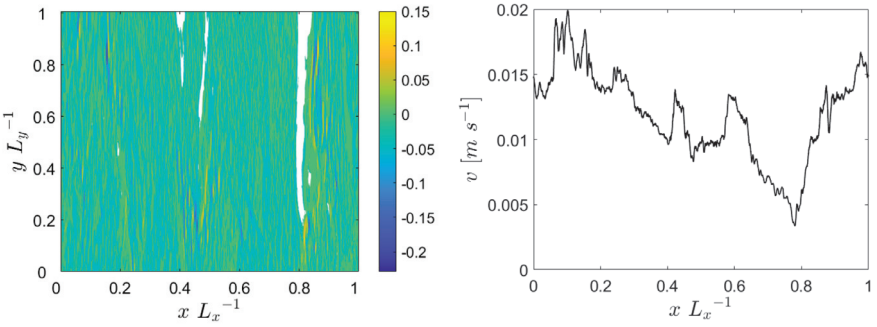

Figure 4: Time and layer averaged meridional velocity distribution (top); time, layer and meridionally-averaged meridional velocity profile vs zonal coordinate (bottom) for the Southern Ocean region in HYCOM simulations.

3. RESULTS

Figure 5 shows angular momentum components resulting from velocity field in HYCOM simulations in the period September 2002 to June 2016, sampled every 30 days. Angular momentum fluctuations are calculated for global oceans and the isolated region of the Southern Ocean and plotted after subtracting the average values in time. As observed in this figure, in contrast to other ocean regions such as North Atlantic and North Pacific [21,22], the fluctuations order of magnitude is the same for the Southern Ocean region and global oceans. This highlights the significant contribution of the Southern Ocean currents in the excitation of polar motion and length of day.

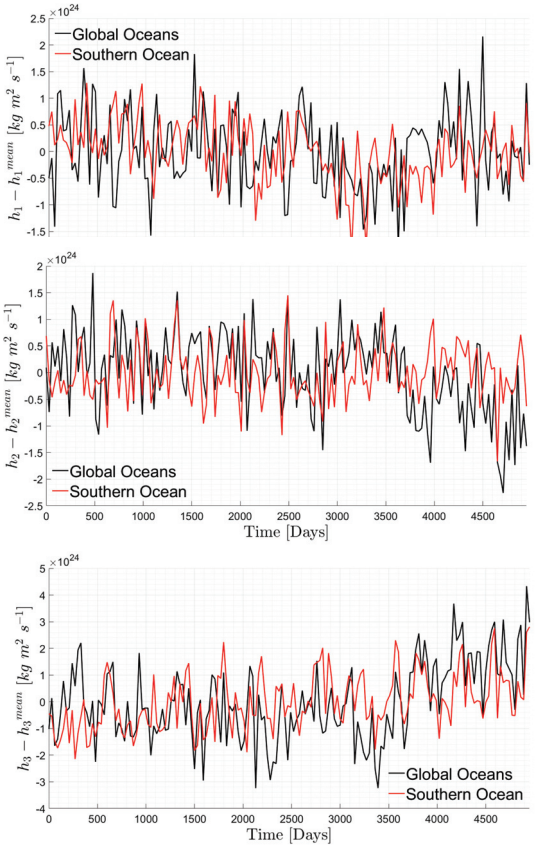

Figure 5: Relative angular momentum components h_1 (top), h_2 (middle) and h_3 (bottom) calculated from the velocity field of the Southern Ocean and global oceans in HYCOM simulations.

Figure 6 shows the change in length of day resulting from angular momentum in the Southern Ocean and global oceans in both time and frequency domains. To analyse the contribution of the Southern Ocean in the excitation of length of day, the correlation factors between the two time series are compared in the original case and after apply low-pass, band-pass and high-pass filters on the signals. In all cases, correlation factors are higher that 0.49 and the highest correlation is observed when a band-pass filter with cut-off frequencies corresponding to 90 days and 400 days are applied on the signals as shown in figure 7.

Figure 8 compares length of day fluctuations caused by global oceans with geodectic observations after subtracting the mass term both in time and frequency domains. Geodetic observations for length of day are obtained from IERS portal and the mass term coefficient (C20) is calculated

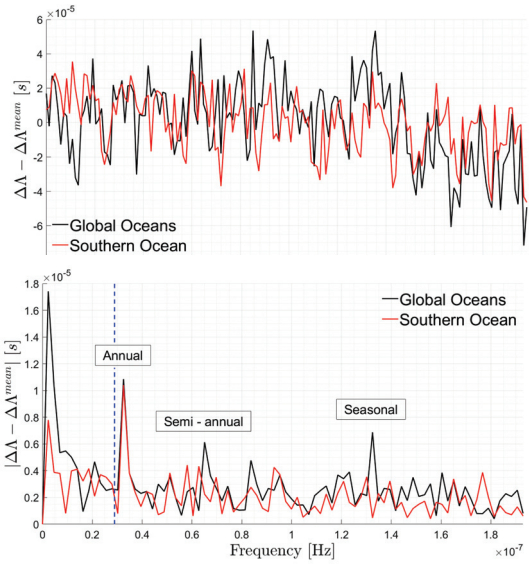

Figure 6: Change in length of day resulting from the Southern Ocean and global oceans angular momentum in HYCOM simulations in time (top) and frequency (bottom) domains. In the bottom panel, the spectral peaks corresponding to seasonal, semi-annual and annual frequencies are labeled accordingly and the frequency of the dashed line corresponds to 400 days.

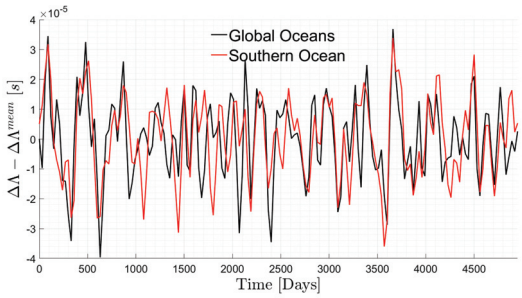

Figure 7: Change in length of day resulting from the Southern Ocean and global oceans angular momentum in HYCOM simulations after applying a band pass filter with cut-off frequencies corresponding to 90 and 400 days

by CNES (French National Centre for Space Studies) using gravimetric Earth observation satellite mission, GRACE (Gravity Recovery A Climate Experiment). The predicted change in length of day by HYCOM simulations is an order of magnitude smaller than the geodetic observations and this can be explained by the dominant effect of atmospheric angular momentum in the excitation of length of day. To examine cross-correlation between the two time series, low-pass, band-pass and high-pass filters were applied on the signals and only in case of a band-pass filter with cut-off frequencies of 90 and 400 days, the correlation factor of 0.2 was observed.

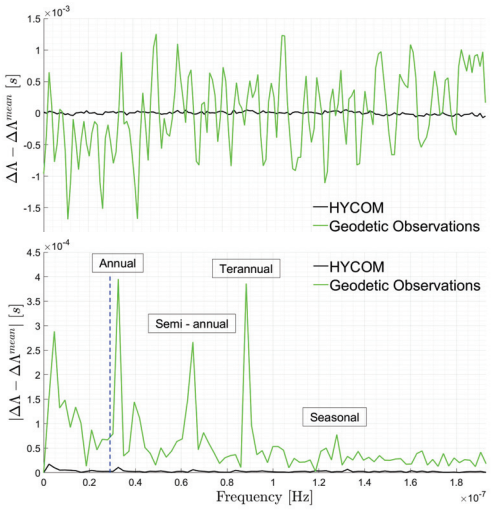

Figure 8: Comparison of length of day fluctuations caused by global oceans in HYCOM simulations with geodectic observations after subtracting the mass term, in time (top) and frequency (bottom) domains.

4. CONCLUSION

In this paper, oceanic excitation of length of day and polar motion are investigated using a high-resolution general circulation ocean model. To this end, oceanic angular momentum components are calculated and compared between the Global Oceans and the isolated region of the Southern Ocean. The comparison shows that the Southern ocean has a dominant contribution in oceanic excitation of polar motion and length of day, supporting previous notions by Wahr [19] and Lambeck and Hopgood [16].Strong correlation between Southern ocean and global oceans is observed in the original time series as well as window-filtered signals with highest correlation in case of band pass filtering with cut-off frequencies corresponding to 90 and 400 days. Excitations from Global oceans have correlation with geodetic observations for motion term when the same band-pass filter is applied i.e. in seasonal or interseasonal scales which agrees with previous studies. One of the important findings of this work is that even when the excitation terms are carefully reconstructed from the high-resolution ocean models, they are not sufficient to explain the geodetic observations. Hence, the future work will concentrate on including the atmospheric angular momentum in the suggested modelling framework.

5. REFERENCES

[1] Seitz, F. and Schmidt, M., 2005. Atmospheric and oceanic contributions to Chandler wobble excitation determined by wavelet filtering. Journal of Geophysical Research: Solid Earth, 110(B11).

[2] Chao, B.F., Ray, R.D., Gipson, J.M., Egbert, G.D. and Ma, C., 1996. Diurnal/semidiurnal polar motion excited by oceanic tidal angular momentum. Journal of Geophysical Research: Solid Earth, 101(B9), pp.20151-20163. Vancouver

[3] Gross, R.S., Fukumori, I. and Menemenlis, D., 2003. Atmospheric and oceanic excitation of the Earth's wobbles during 1980–2000. Journal of Geophysical Research: Solid Earth, 108(B8).

[4] Dicke, R.H., 1961. The Rotation of the Earth (A geophysical discussion).

[5] Nastula, J., Salstein, D.A. and Gross, R., 2014. Regional multi-fluid-based geophysical excitation of polar motion. In Earth on the Edge: Science for a Sustainable Planet (pp. 467-472). Springer, Berlin, Heidelberg.

[6] McCarthy, D.D. and Luzum, B.J., 1991. Prediction of Earth orientation. Bulletin g´eod´esique,

65(1), pp.18-21.
[7] Gross, R.S., 2000. The excitation of the Chandler wobble. Geophysical Research Letters, 27(15), pp.2329-2332.
[8] Aoyama, Y. and Naito, I., 2001. Atmospheric excitation of the Chandler wobble, 1983–1998. Journal of Geophysical Research: Solid Earth, 106(B5), pp.8941-8954.
[9] Brzezi´nski, A. and Nastula, J., 2002. Oceanic excitation of the Chandler wobble. Advances in Space Research, 30(2), pp.195-200.
[10] Gross, R.S., 2007. Earth rotation variations-long period. Treatise on geophysics, 3, pp.239-294.
[11] Schindelegger, M., Salstein, D., Ein˘spigel, D. and Mayerhofer, C., 2017. Diurnal atmosphere[U+2010]ocean signals in Earth's rotation rate and a possible modulation through ENSO. Geophysical Research Letters, 44(6), pp.2755-2762.
[12] Gross, R.S., Fukumori, I., Menemenlis, D. and Gegout, P., 2004. Atmospheric and oceanic excitation of length of day variations during 1980–2000. Journal of Geophysical Research: Solid Earth, 109(B1).
[13] Johnson, T.J., Wilson, C.R. and Chao, B.F., 1999. Oceanic angular momentum variability estimated from the Parallel Ocean Climate Model, 1988–1998. Journal of Geophysical Research: Solid Earth, 104(B11), pp.25183-25195.
[14] Rosen, R.D. and Salstein, D.A., 1985. Contribution of stratospheric winds to annual and semiannual fluctuations in atmospheric angular momentum and the length of day. Journal of Geophysical Research: Atmospheres, 90(D5), pp.8033-8041.
[15] Dill, R., Dobslaw, H. and Thomas, M., 2019. Improved 90-day Earth orientation predictions from angular momentum forecasts of atmosphere, ocean, and terrestrial hydrosphere. Journal of Geodesy, 93(3), pp.287-295.
[16] Lambeck, K. and Hopgood, P., 1981. The Earth's rotation and atmospheric circulation, from 1963 to 1973. Geophysical Journal International, 64(1), pp.67-89.
[17] Ma J., Zhou Y.H., Liao D.C., Chen J.L., 2009. Excitation of Chandler wobble by Pacific, Indian and Atlantic Oceans from 1980 to 2005, Chinese Journal of Astronomy and Astrophysics, 33(4), 410–420.
[18] Nastula J., Gross R.S., Salstein D.A., 2012. Oceanic excitation of polar motion: identification of specific oceanic areas important for polar motion excitation, Journal of Geodynamics., 62, 16–23.
[19] Wahr J.M., 1983. The effects of the atmosphere and oceans on the Earth's wobble and on the seasonal variations in the length of day – II. Results, Geophysical Journal International, 74(2), 451–487.
[20] Wallcraft, A.J., Metzger, E.J. and Carroll, S.N., 2009. Software design description for the HYbrid Coordinate Ocean Model (HYCOM) version 2.2. Naval Research Laboratory, pp.13-15.
[21] Naghibi, S.E., Jalali, M.A., Karabasov, S.A. and Alam, M.R., 2017. Excitation of the Earth's Chandler wobble by a turbulent oceanic double-gyre. Geophysical Journal International, 209(1), pp.509-516.
[22] Naghibi, S.E. and Karabasov, S.A., 2020. Excitation of the Earth's Chandler wobble by the North Atlantic double-gyre. Astrometry, Earth Rotation, and Reference Systems in the GAIA era, pp.237-242.
[23] Naghibi, S.E., Karabasov, S.A., Jalali, M.A. and Sadati, S.H., 2019. Fast spectral solutions of the double-gyre problem in a turbulent flow regime. Applied Mathematical Modelling, 66, pp.745-767.
[24] Naghibi, S.E., Karabasov, S.A. and Kamenkovich, I., 2023. Zonal jets in the Southern Ocean: A semi-analytical model based on scale separation. Ocean Modelling, 183, p.102198.
[25] Gross, R.S., 2007. Earth rotation variations-long period. Treatise on geophysics, 3, pp.239-294.